Design and cold test of a rectangular cavity beam position monitor

SU Jia-Hang(苏佳杭)[1,2;1)] DU Ying-Chao(杜应超)[1,2] HUA Jian-Fei(华剑飞)[1,2]
ZHENG Shu-Xin(郑曙昕)[1,2] QIU Jia-Qi(裘家琪)[1,2] YANG Jin(杨晋)[1,2]
HUANG Wen-Hui(黄文会)[1,2] CHEN Huai-Bi(陈怀璧)[1,2] TANG Chuan-Xiang(唐传祥)[1,2]

[1] Department of Engineering Physics, Tsinghua University, Beijing 100084, China
[2] Key Laboratory of Particle & Radiation Imaging (Tsinghua University), Ministry of Education, Beijing 100084, China

Abstract: The CBPM is a kind of monitor which is used for the measurement of beam transverse position. It is becoming increasingly popular due to its high potential in resolution performance. In theory, the resolution can reach about 1 nanometer. In this paper, a rectangular CBPM is designed for it has better X-Y isolation than a cylindrical one. It has been simulated and measured, and the results agree with each other very well. The procedures and results for the simulation and the cold test will be shown later and it will be proved that this is a reliable method for the CBPM design.

Key words: CBPM, resolution, physical design, dipole mode, $Q_{\rm ext}$, cold test

PACS: 29.27.Fh, 29.27.Eg **DOI:** 10.1088/1674-1137/37/1/017002

1 Introduction

BPMs (beam position monitors) are now widely used in injectors, storage rings, linacs, linear colliders, and undulators of FELs to ensure that the electron beam moves along the right trajectory, and the CBPM offers another method to measure the beam transverse position compared with the stripline BPM. When a bunch passes through the cavity, the eigenmodes of the electromagnetic field will be excited by the Wakefield effect. The mode whose amplitude is proportional to the beam offset value is coupled through the waveguide and then coupled out through the feedthrough. Thus the output signal reflects the offset information and can be treated as the offset value multiplied by a constant. We now prefer CBPMs to stripline BPMs because of their high resolution potential. For a stripline BPM, the signal is the difference between the voltages of the opposite electrodes, which are caused by the offset beam. Thus if the beam is near the axis, the difference will be very small and many significant digits will surely be lost. This will certainly limit the theoretical resolution, and it can only reach several microns. But it will no longer be a problem in CBPMs, for the signals from the opposite ports are the same, thus we can get higher position resolution by using a CBPM.

The most commonly used CBPMs now are cylindrical ones, which are easy to design and make. Many labs have designed cylindrical CBPMs whose resolution have reached micron and even sub-micron levels [1–8]. However, because of processing limits, for a cylindrical CBPM, the transverse section will always be an elliptical one. So when it is used to measure the transverse position of one beam, the signal in one direction will probably contain the beam offset information of both directions, and this will of course make the resolution lower (Fig. 1). It will no longer be a problem in a rectangular one, for the rectangular CBPM has better X-Y isolation and thus limit theoretical resolution better than a cylindrical one [9]. The best resolution ever obtained is 8.72 nm by the rectangular CBPM designed by KEK, which is very close to the theoretical value [10].

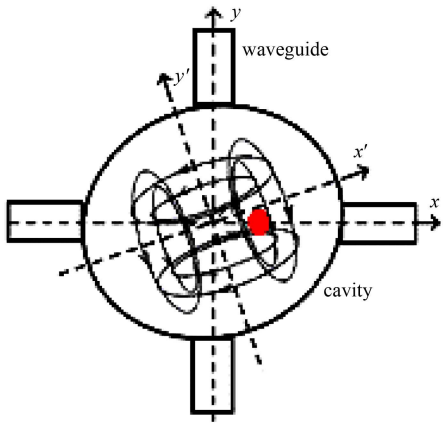

Fig. 1. The eigenmodes in an ellipse cavity.

Received 2 March 2012
1) E-mail: sujh06@163.com
©2013 Chinese Physical Society and the Institute of High Energy Physics of the Chinese Academy of Sciences and the Institute of Modern Physics of the Chinese Academy of Sciences and IOP Publishing Ltd

In the Tsinghua Thomson scattering X-ray source [11], it is necessary to set BPMs to monitor the beam transverse position, and this leads to the design of our rectangular CBPM. As a prototype CBPM, the resolution is expected to reach 500 nm first at the bunch charge of 1 nC.

2 Design and simulation results for the rectangular CBPM

2.1 Physical design of the CBPM

For the rectangular cavity, the monopole mode is TM110, whose amplitude is only proportional to the bunch charge. It will be cut-off by the waveguide and can be only used in the reference cavity. The dipole modes are TM210 and TM120, respectively for the horizontal and vertical beam offset. Their amplitude is not only proportional to the bunch charge, but also related to the beam offset, and when the offset is small, the amplitude can be treated to be proportional to the offset value. This is the useful signal for the transverse position measurement. Furthermore, the X-offset information will be detected from the vertical ports, while the Y offset information detected from the horizontal ports (Fig. 2).

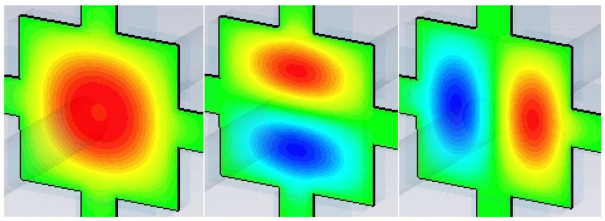

Fig. 2. The TM110 mode, TM210 mode and TM120 mode in the rectangular cavity.

Take the X-offset for example, it will excite the TM210 mode, and this mode will couple into the vertical waveguide with the TE10 mode. So the X-offset signal will be detected from the vertical ports, and it is the same for the Y-offset.The target frequencies are 5.6525 GHz and 5.7715 GHz respectively for the horizontal and vertical designs with the structure shown in Fig. 3.

The size needed in the cavity design is shown in Fig. 4. The offset passing beam excites eigenmodes in the cavity, and the frequencies of the eigenmodes are related to a, b and cl. Some of the exciting modes will come into the waveguides by coupling, which are usually distinguished as dipole modes and high order modes. What we need is just dipole modes, so proper w1 has to be set to attenuate the high order modes. Besides, some exciting modes will also come into the waveguides because of the mode-leak effect, where the monopole mode contributes most. So wa and wb need to be set properly to ensure that the cut-off frequency of the waveguide comes between the monopole mode frequency and the dipole mode frequency. To get higher amplitude and higher attenuation length of the output signal voltage, we prefer lower $Q_{\rm ext}$, which is decided by wrx, wry and wd.

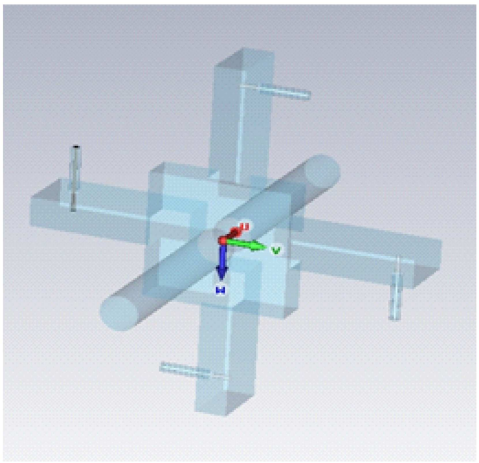

Fig. 3. The structure of the CBPM.

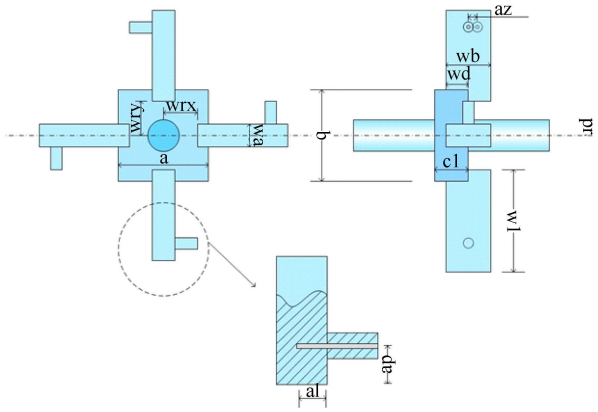

Fig. 4. The sizes of cavity design.

Thus at the exit port of the waveguide, where we set the feedthrough, there is only the information about dipole mode and this information will be extracted from the feedthrough to the post-processing circuit. The process from the cavity to the waveguide is often called first-stage coupling, and the process between the waveguide and the feedthrough called the second-stage process. So if we want to get the same $Q_{\rm ext}$ from the second-stage coupling compared with the first-stage coupling, we should optimize az, ap and al to get the reflection as low as possible.

Furthermore, we should set proper pr to get a balance between the mode-leak effect and the beam loss. Larger pr means lower beam loss but also higher mode-leak effect. The finished size of the design is shown in Table 1.

Table 1. The finished size of the design.

symbol	value/mm	symbol	value/mm
a	56.66	wl	60
b	54.654	wd	11.25
cl	15	wry	16
pr	7.5	wrx	17
wa	28.5	ap	16
wb	12.6	al	8.39

2.2 Simulation results for the CBPM

2.2.1 Frequency

With the current a and b, and taking chamfering and cavity material into consideration, we can get the simulation value of the dipole mode frequencies. The frequency of the TM210 mode is 5.6666 GHz and the frequency of the TM120 mode is 5.7846 GHz.

2.2.2 Q-value

As shown in Fig. 5, we can take the CBPM as a lossless model.

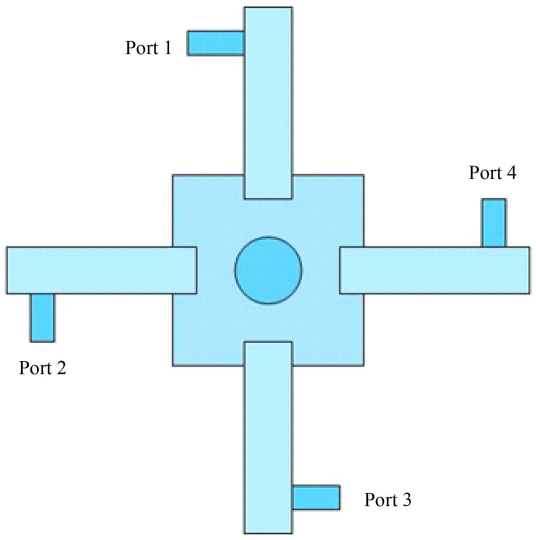

Fig. 5. Port model of the CBPM.

Because of the good X-Y isolation, we can divide the model into two two-port network models, which is shown below.

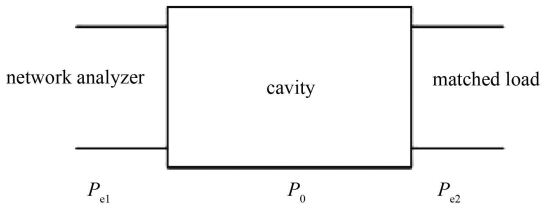

Fig. 6. Two-port network model.

Thus the $Q_{\rm L}$ we get from simulation can be described as

$$Q'_{\rm L}=\frac{\omega U_0}{P_0+P_{\rm e1}+P_{\rm e2}}, \tag{1}$$

where $P_{\rm e1}$ and $P_{\rm e2}$ are the energy coupling out in the two opposite waveguides and $P_{\rm e1}\approx P_{\rm e2}=P_{\rm e}$. Thus the equivalent intrinsic quality factor can be defined as

$$Q_0^*=\frac{\omega U_0}{P_0+P_{\rm e}}, \tag{2}$$

so the equivalent coupling coefficient is

$$\beta^*=\frac{Q_0^*}{Q_{\rm e}}=\frac{P_{\rm e}}{P_0+P_{\rm e}}. \tag{3}$$

Thus the real intrinsic quality factor can be expressed as

$$\begin{aligned} Q_0 &= \frac{\omega U_0}{P_0}=\frac{\omega U_0}{P_0+2P_{\rm e}}\times\frac{P_0+2P_{\rm e}}{P_0} \\ &= Q'_{\rm L}\times\left(1+\frac{2}{\frac{1}{\beta^*}-1}\right)=Q'_{\rm L}\times\left(\frac{1+\beta^*}{1-\beta^*}\right), \end{aligned} \tag{4}$$

and the external quality factor

$$\begin{aligned} Q_{\rm ext} &= \frac{\omega U_0}{P_{\rm e}}=\frac{\omega U_0}{P_0+2P_{\rm e}}\times\frac{P_0+2P_{\rm e}}{P_{\rm e}} \\ &= Q'_{\rm L}\times\left(2+\frac{1}{\beta^*}-1\right)=Q'_{\rm L}\times\left(\frac{1+\beta^*}{\beta^*}\right). \end{aligned} \tag{5}$$

So the simulation results of the Q-values can be described as shown in Table 2.

Table 2. Simulation results of the Q-values.

	TM210	TM120
Q_0	9707.5	9700.4
$Q'_{\rm L}$	1645.7	1464
β^*	0.71	0.737
$Q_{\rm ext}$	3963.292	3451.291

Where $Q_{\rm ext}$ is the single port external quality factor.

2.2.3 X-Y isolation and monopole mode leak simulation

In theory, a rectangular CBPM performs well in X-Y isolation and monopole mode leak cut-off.

From the simulation results, it is easy to see that the X-Y isolation is about -50 dB, it means that the neighbouring ports can be ignored if one port is taken into measurement. Take Fig. 7 for example.The mode excited from the vertical port only leaks e-5 into the neighbouring port, and this will make little sense to the output signal from the horizontal port.

It is the same for monopole mode leak cut-off. From Fig. 8 we can see that the attenuation is <-110 dB and the monopole leak is so slight that it can be ignored.

2.2.4 Theoretical resolution calculation

When the bunch passes through the cavity, it will excite different eigenmodes. Let us assume a Gaussian distribution in beam direction with beam size σ_z, the exciting voltage is the integral of the electric field along

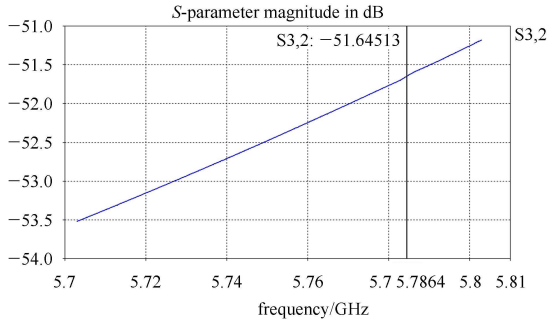

Fig. 7. The simulation results of X-Y isolation.

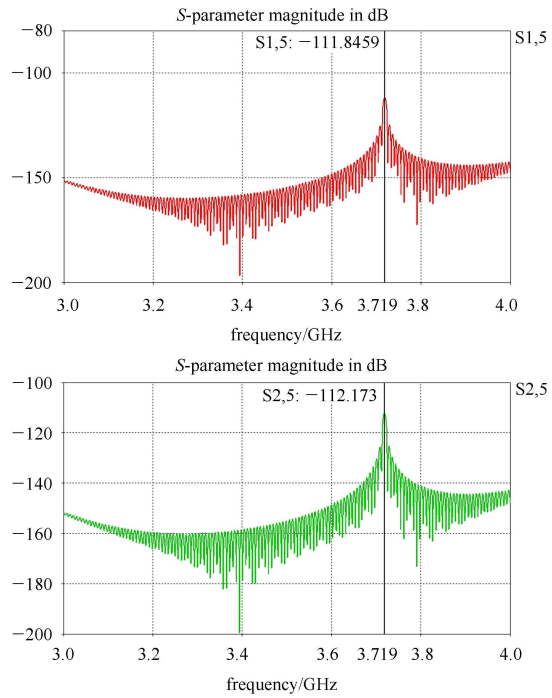

Fig. 8. The simulation results of monopole mode leak cut-off.

the bunch trajectory and can be expressed as [12]

$$V_{\rm p0}=\frac{q\omega_n}{2}\sqrt{(R/Q)_n\frac{Z}{Q_{\rm ext}}}\exp\left(-\frac{\omega^2\sigma_z^2}{2c^2}\right). \tag{6}$$

where $(R/Q)_n$ is the normalized shunt impedance of the n th eigenmode, Z is the output impedance and is 50 Ω in usual.

The normalized shunt impedance R/Q characterizes the strength of the exchanging energy between the bunch and the cavity. It depends only on the cavity shape and size, not on the cavity material or surface condition. R is the shunt impedance. It represents the accelerating efficiency of the cavity and is shown as

$$R=\frac{|V|^2}{P_{\rm wall}}=\frac{\left|\int E{\rm d}s\right|^2}{P_{\rm wall}}, \tag{7}$$

where $P_{\rm wall}$ is the power lost in the cavity because of the imperfections of the cavity wall. So with the definition of Q_0

$$Q_0=\frac{\omega U}{P_{\rm wall}}, \tag{8}$$

where U is the energy storage in the cavity. The R/Q can be written as

$$(R/Q)_n=\frac{|V_n|^2}{\omega U}. \tag{9}$$

So U can be expressed as

$$U=\frac{|V_n|^2}{\omega_n(R/Q)_n}=\frac{q^2\omega_n}{4}(R/Q)_n\exp\left(-\frac{\omega_n^2\sigma_z^2}{c^2}\right). \tag{10}$$

With the definition of $Q_{\rm ext}$,

$$Q_{\rm ext}=\frac{\omega U}{P_{\rm out}}, \tag{11}$$

the output signal of the n-th eigenmode can be shown as

$$\begin{aligned}V_{\rm outn}&=\sqrt{P_{\rm outn}Z}=\sqrt{\frac{\omega_n U}{Q_{\rm ext}}Z}\\&=\frac{q\omega_n}{2}\sqrt{\frac{Z}{Q_{\rm ext}}(R/Q)_n}\exp\left(-\frac{\omega_n^2\sigma_z^2}{2c^2}\right).\end{aligned} \tag{12}$$

For a rectangular cavity, take TM210 mode for example, the normalized shunt impedance can be written as

$$\begin{aligned}\frac{R}{Q}&=\frac{|V|^2}{\omega U}=\frac{\left|\int_{-L/2}^{L/2}\left[E_0\sin\left(\frac{2\pi}{a}x\right)\sin\left(\frac{\pi}{b}y\right){\rm e}^{{\rm j}\omega t}\right]{\rm d}z\right|^2}{\omega\int\frac{1}{2}\varepsilon\left|E_0\sin\left(\frac{2\pi}{a}x\right)\sin\left(\frac{\pi}{b}y\right){\rm e}^{{\rm j}\omega t}\right|^2{\rm d}V}\\&=\frac{8LT^2\sin^2\left(\frac{2\pi}{a}x\right)\sin^2\left(\frac{\pi}{b}y\right)}{\omega\varepsilon ab},\end{aligned} \tag{13}$$

where T=sin($\omega L/2c$)/($\omega L/2c$). Considering that the beam passes the vertical center and has a slight offset in the horizontal plane, it can be known that

$$R/Q\approx\frac{8LT^2}{\omega\varepsilon ab}\left(\frac{2\pi}{a}x\right)^2. \tag{14}$$

So considering the bunch to be short enough, the TM210 mode output signal voltage amplitude can be written as

$$V_{210}=\frac{q\omega_{210}}{2}\sqrt{\frac{Z}{Q_{\rm ext210}}\frac{8LT^2}{\omega_{210}\varepsilon ab}}\frac{2\pi}{a}x. \tag{15}$$

It is the same for the TM120 mode and the output voltage is

$$V_{120}=\frac{q\omega_{120}}{2}\sqrt{\frac{Z}{Q_{\rm ext120}}\frac{8LT^2}{\omega_{120}\varepsilon ab}}\frac{2\pi}{b}y. \tag{16}$$

In the ideal situation, the definition of the theoretical resolution is the offset value which makes the output signal voltage of the beam offset equal to the signal voltage of the thermal noise. And the equivalent thermal noise can be expressed as

$$V_{\rm N}=\sqrt{4kT\Delta BRN_{\rm F}}, \tag{17}$$

where k is the Boltzman constant, T is the absolute temperature, ΔB is the bandwidth of the head amplifier, R is the circuit resistance, and $N_{\rm F}$ is the noise figure of the head amplifier.

Only considering the thermal noise, we can evaluate the resolution as ∼4.5 nm@1 nC for the horizontal plane and ∼4.1 nm@1 nC for the vertical plane assuming the noise figure of 3 dB in the head amplifier. In the practical setup [2], by including the signal losses of cables, magic-T, filter, attenuator, mixer and waveform shaping loss in filters, the total signal loss can be −20 dB.Thus, the expected resolution becomes as ∼45 nm@1 nC for the horizontal plane and ∼41 nm@1 nC for the vertical plane.

3 Cold test results for the CBPM

The cold test model is shown in Fig. 9. Fig. 9(a) is the assembled model of the CBPM, Fig. 9(b) is the main cavity, Fig. 9(c) is the front cover and Fig. 9(d) is the welded model. With this model, we perform the cold test and get a reasonable result which agrees with the design target well.

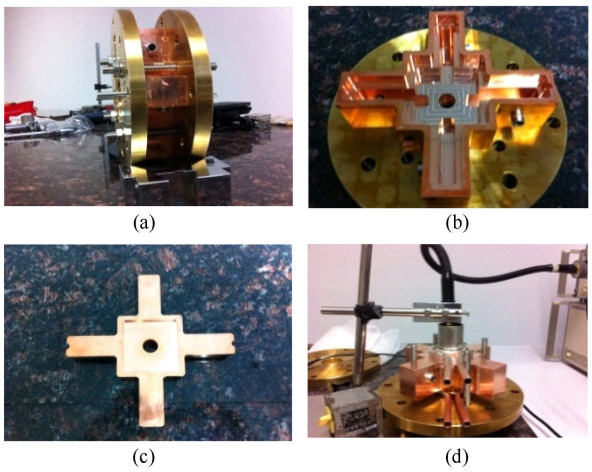

Fig. 9. The CBPM cold test model.

The cavity is first tested with the final size and then optimized to meet the target frequencies. 0.12 mm and 0.086 mm corrections are made, respectively, for the horizontal and the vertical designs. The main cavity and the front cover are then welded together and the final cold test is performed.

3.1 Frequency

The measured frequencies are 5.6618 GHz and 5.7794 GHz, respectively, for TM210 mode and TM120 mode with the final size. Compared with the simulation results, it is easy to see that the cold test ones are lower. This is caused by the imperfections brought in the mechanical process, such as matching errors, size tolerance, and so on. Furthermore, as the component is processed by milling, the surface roughness will certainly bring in more errors compared with a lathed one. Fortunately, this will not influence the relation between the change of the cavity size and the change of the frequency. As simulated, if we change a by 0.01 mm, the frequency of the TM210 mode will decrease by about 700 kHz while the frequency of the TM120 mode will decrease only by about 200 kHz. This is nearly the same for b. So we can change a and b to get the proper frequencies at last.

After welding, the measured frequencies are 5.653075 GHz and 5.77195 GHz, respectively, for TM210 mode and TM120 mode. With the target frequencies, the cold test target frequencies can be written as [13]

$$f_{\rm c}=f_{\rm v}(1-(n-1)\times10^{-6}+(T_{\rm v}-T_{\rm c})\times g), \tag{18}$$

where v means vacuum and c means cold test. Besides, n is the refractive index and g is the linear expanding factor of the oxygen-free copper. So the cold test target frequencies are 5.652905 GHz and 5.771914 GHz, respectively, for TM210 mode and TM120 mode. The cold test results match the theoretical ones very well.

3.2 Q_0

For the position cavity, higher Q_0 is preferred because it means lower power loss in the cavity. With the final size, the measured Q_0 is ∼6500 while the designed target is ∼9700. It means that we only reach ∼67% of the target value. This is not an ideal result but still a reasonable one. First, as the model has not been welded and the fixture could not ensure optimum tightness, some electromagnetic field will leak through the slot; this will increase the power of energy loss but will be compensated after being welded. Furthermore, the milling surface enlarges the surface of the cavity, which will surely increase the wall energy loss. This value is unpredictable and cannot be avoided. After welding, the value of Q_0 increases and reaches ∼8000, which satisfies our requirements.

3.3 $Q_{\rm e}$

In reality, we prefer lower $Q_{\rm e}$ to get higher output signal voltage and better position resolution. The measured $Q_{\rm e}$s are ∼4000 and ∼3500, respectively, for TM210 mode and TM120 mode, compared with 3963.292 and 3451.291 from simulation. The cold test result is nearly the same as simulation and remains nearly unchanged after welding, which are ∼3400 and ∼2900, respectively,

for TM210 mode and TM120 mode.

3.4 *X-Y* isolation

In the cold test, we use the transport method to measure the relative isolation. The results are shown in Table 3 and Table 4.

Table 3. X-Y isolation measurement.

exciting port	4	3
S14(S13)	−37 dB	−3.6 dB
S24(S23)	−3.5 dB	−40.8 dB
S34(S43)	−41 dB	−34.8 dB
X-Y isolation	−35.5 dB	−34.2 dB

Table 4. X-Y isolation measurement after welding.

exciting port	4	3
S14(S13)	−36.6 dB	−2.2 dB
S24(S23)	−1.67 dB	−36.1 dB
S34(S43)	−42.9 dB	−39.7 dB
X-Y isolation	∼−36 dB	∼−34 dB

It is easy to see that only about 0.03% of the energy of the injecting microwave couples out to the neighbouring port.

3.5 Monopole mode leak

In theory, the monopole mode leak level is very low, not only because that the monopole mode can not couple into the waveguide with any mode, but also because the frequency is lower than the cut-off frequency of the waveguide. So even though there is some monopole mode coupling into the waveguide because of the slight bent field existing at the waveguide port, it would be attenuated quickly. However, in reality, the waveguides will not be totally perfect; there will still be some monopole mode coupled out of the feeedthrough. The measured attenuation of the monopole mode in each port is shown below.

Table 5. Attenuation of the monopole mode.

exciting attenuation	−7.7 dB	relative attenuation
Port1 attenuation	−86 dB	−78.3 dB
Port2 attenuation	−81 dB	−73.3 dB
Port3 attenuation	−81.6 dB	−73.9 dB
Port4 attenuation	−82 dB	−74.3 dB

It means that only about 3E-8 of the energy of the monopole mode will couple out through the feedthrough. Comparing this with the simulation results, it is easy to see that in the actual component the attenuation is not as good as the one in the ideal model, which is because of the imperfections in the CBPM. However, this contributes little to the dipole mode measurement and can be ignored.

Furthermore, the measured attenuation of the monopole mode after welding in each port is shown below.

Table 6. Attenuation of the monopole mode after welding.

exciting attenuation	−0.12 dB	relative attenuation
Port1 attenuation	−82.5 dB	−82.38 dB
Port2 attenuation	−77.6 dB	−77.48 dB
Port3 attenuation	−74.9 dB	−74.78 dB
Port4 attenuation	−73.6 dB	−73.48 dB

Comparing this with the former ones, the monopole attenuation also remains the same.

4 Conclusion

In this paper, the design process of a rectangular CBPM is shown, and the cold test results agree with the simulation very well. So we have obtained a reliable method for rectangular CBPM design which is expected to provide good resolution and good performance. Furthermore, further hot testing will be done later to get the real resolution.

References

1 Slaton T et al. Development of Nanometer Resolution C-band Radio Frequency Beam Position Monitors in the Final Focus Test Beam. LINAC'98. Chicago. KEK Preprint, Aug. 1998. 98–145

2 Shintake T. Development of Nanometer Resolution RF-BPM. KEK Preprint, November 1998. 98–188

3 Balakin V et al. Experimental Results From a Microwave Cavity Beam Position Monitor. Proceedings of the 1999 Particle Accelerator Conference. New York. 1999

4 Johnson R et al. Cavity BPMs for the NLC. SLAC-PUB-9211, May 2002

5 LI Zeng-Hai et al. Cavity BPM with Dipole-mode-selective Coupler. Proceedings of the 2003 Particle Accelerator Conference. 2003

6 Walston S et al. Nuclear Instruments and Methods in Physics Research A, 2007, **578**: 1–22

7 Walston S et al. Resolution of a High Performance Cavity Beam Position Monitor System. Proceedings PAC. 2007

8 CHU Jian-Hua. Development of a C-Band Cavity BPM and RF Electronics (Doctoral Thesis). Shanghai: Shanghai Institute of Applied Physics, 2008 (in Chinese)

9 LI Xiang. Design and Experiments for Cavity Beam Position Monitor (Master Thesis). Department of Engineering Physics, Tsinghua University, May, 2009

10 Yoichi Inoue et al. Physical Review Special Topics-Accelerators and Beams, 2008, **11**: 062801

11 TANG Chuan-Xiang et al. Nuclear Instruments and Methods in Physics Research A, 2009, **608**: S70–S74

12 Tomoya Nakamura. Development of Beam-position Monitors with High Position Resolution (Master Thesis). Department of Physics, Graduate School of Science, The University of Tokyo, Feb. 3, 2008

13 HE Xiao-Zhong. Theoratical and Initial Experimental Research on Low Emittance Photoinjector (Doctor Thesis). Department of Engineering Physics, Tsinghua University, June, 2006